Materials Research Proceedings 38 (2023) 67-77 https://doi.org/10.21741/9781644902837-11

Effect of Hot Isostatic Pressing on Microstructure and Properties of GH4169 Superalloy Manufactured by SLM

Shanting Niu[1,a], Hongpeng Xin[1,b], Lida Che[1,c*], Haofeng Li[1,d], Xiangyang Li[2,e]

[1]CISRI HIPEX, Haidian District, Beijing, P. R. China

[2]CISRI, Haidian District, Beijing, P. R. China

[a]niushanting@hipex.cn, [b]xinhongpeng@hipex.cn, [c]chelida@hipex.cn, [d]lihaofeng@hipex.cn, [e]lix y@cisri.com.cn

Keywords: Hot Isostatic Pressing (HIP), Additive Manufacturing, GH4169, Properties

Abstract. Superalloy GH4169 is an extremely important material for aircraft structural components in aero-engines. In this study, the effects of different hot isostatic pressing temperature and pressure on the microstructure and mechanical properties of GH4169 were studied by means of metallographic microscope, scanning electron microscope and tensile experiment. The results show that hot isostatic pressing can significantly improve the microstructure of the test alloy manufactured by SLM. With the increase of hot isostatic pressing temperature and pressure, the tensile strength and yield strength of the test alloy decreased slightly, while the elongation showed an opposite trend. The increase of elongation is attributed to the improvement of microstructure uniformity of the test alloy by hot isostatic pressing.

1. Introduction

As the service requirements of aviation, aerospace and nuclear industry materials become more and more demanding, conventional materials have been unable to meet the requirements. At this time, the emergence of nickel-based superalloys that can maintain mechanical properties at high temperatures to meet these requirements [1]. Of nickel-based superalloy GH4169 was investigated at 650℃ has high yield strength, good corrosion resistant ability and good high temperature oxidation resistance, etc., applicable to the manufacture of low temperature and under 650℃ of rocket engine, aviation and ground gas turbine engine components, is currently the most widely used in aerospace field of high temperature alloy[2,3]. The alloy is a Ni-Cr-Fe base precipitation strengthening superalloy, which consists of γ matrix, γ' and γ'' phase, δ phase and carbide[4]. The traditional manufacturing methods of GH4169 alloy are precision casting, forging and subsequent machining, etc[5]. However, this method has some problems such as low material utilization rate, low production efficiency, high processing cost and difficulty in forming three-dimensional complex structure, which greatly limits the application scope of the alloy.

Selective laser melting is one of the most widely studied and applied metal additive manufacturing technologies. Its working principle is that the metal powder is scanned layer by layer by high-energy laser beam according to the path planned by digital model slice[6]. The metal powder is melted and solidified under the action of laser energy and deposited layer by layer, thus realizing the rapid manufacturing of parts[7]. Compared with the traditional manufacturing technology, this technology has the advantages of high design freedom, one-time forming of complex parts, high material utilization rate, excellent finished product performance, and has significant advantages in preparing three-dimensional complex superalloy parts[8]. However, the results show that the GH4169 alloy samples prepared by SLM process usually contain defects such as porosity and non-fusion, and there are significant differences in the transverse and longitudinal microstructure[9,10]. There are a large number of Laves harmful phases in the micro-segregation of the molten pool solidification microstructure [11,12].

Materials Research Proceedings 38 (2023) 67-77 https://doi.org/10.21741/9781644902837-11

HIP is an effective method to eliminate defects using high temperature and high pressure. Studies show that this method can effectively eliminate cracks, holes and non-fusion defects in GH4169 alloy, which has been widely concerned in the world [13]. SH Chang et al. conducted HIP treatment on Inconel718 alloy castings at different temperatures, pressures and holding time, and heat treated the corresponding samples, and then tested the tensile properties of the samples at room temperature and high temperature under different experimental conditions. The optimum HIP parameters of Inconel718 casting was determined to be 1180℃-175MPa-4h [5]. At present, there have been many studies on the HIP treatment of additive manufacturing GH4169/IN718 alloy, but the HIP process used in the present study is single, lack of studies on the influence of different HIP temperature and pressure on the microstructure and mechanical properties of SLM manufacturing GH4169 alloy. Therefore, in order to meet the requirements of engineering application, this paper studied the influence of SLM on the microstructure and mechanical properties of GH4169 alloy, and found out the more ideal process parameters of HIP.

2. Experimental

The experimental material is GH4169 alloy powder prepared by gas atomization method in electrode induction melting, and the protective gas is argon. The morphology of the powder is shown in Fig. 1, and the particle size is 15-53 μm. Fine satellite particles can be observed attached to the main particles. The particle size distribution of D10=21.9μm, D50=33.9μm, D90=52.2μm was measured by Malvern laser particle size analyzer.

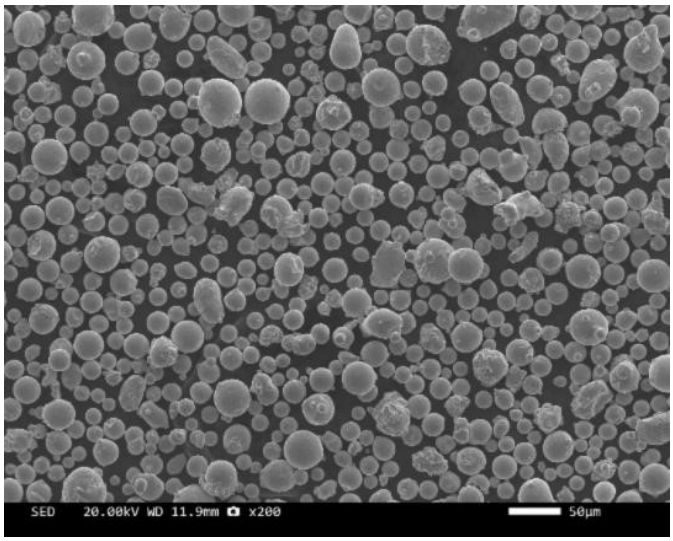

Figure 1. GH4169 powder morphology

Table 1. Chemical Composition of GH4169 alloy powder [Mass Fraction,%]

Element	Ni	Nb	Mo	Cr	Al	Ti	Co	B
Content	53.03	4.98	3.10	18.64	0.42	0.81	0.053	＜0.005
Element	Si	Mn	Cu	Mg	C	S	P	Fe
Content	0.056	＜0.003	0.08	＜0.005	0.015	＜0.003	＜0.005	Bal.

In this experiment, FS271M equipment of Hua Shu High-tech was used for SLM forming of the sample, which was used to directly print the rod sample for mechanical properties testing. The sample size is φ10mm×100mm, forming direction along the sample axial vertical substrate. The

Materials Research Proceedings 38 (2023) 67-77 https://doi.org/10.21741/9781644902837-11

main forming parameters are shown in Table 2, strip printing strategy is adopted (as shown in Fig. 2). and the printed delivery sample is shown in Fig. 3.

Table 2. Forming parameters of GH4169 alloy SLM

Laser power[W]	Scanning speed[mm·s^{-1}]	Thickness[μm]	Scanning interval[μm]
400	2700	30	80

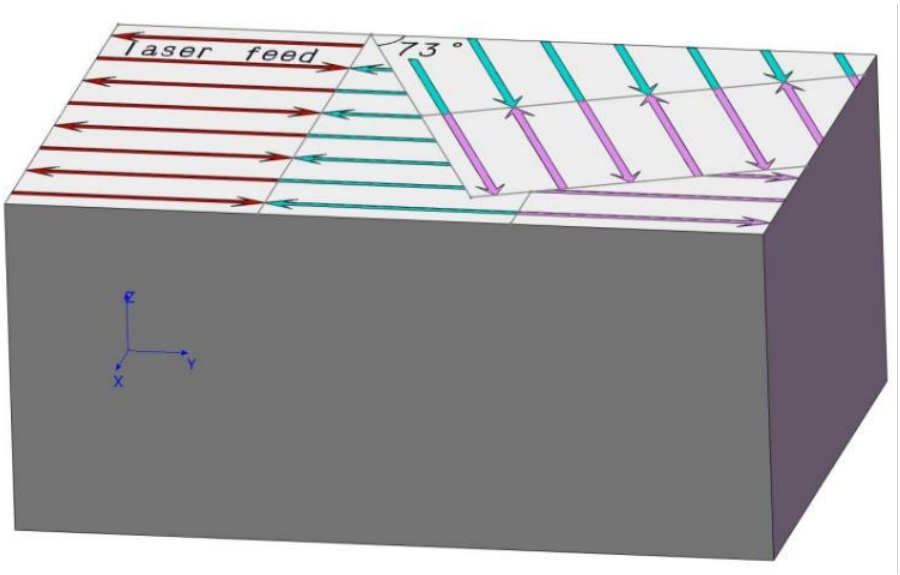

Figure 2. Schematic diagram of strip printing strategy

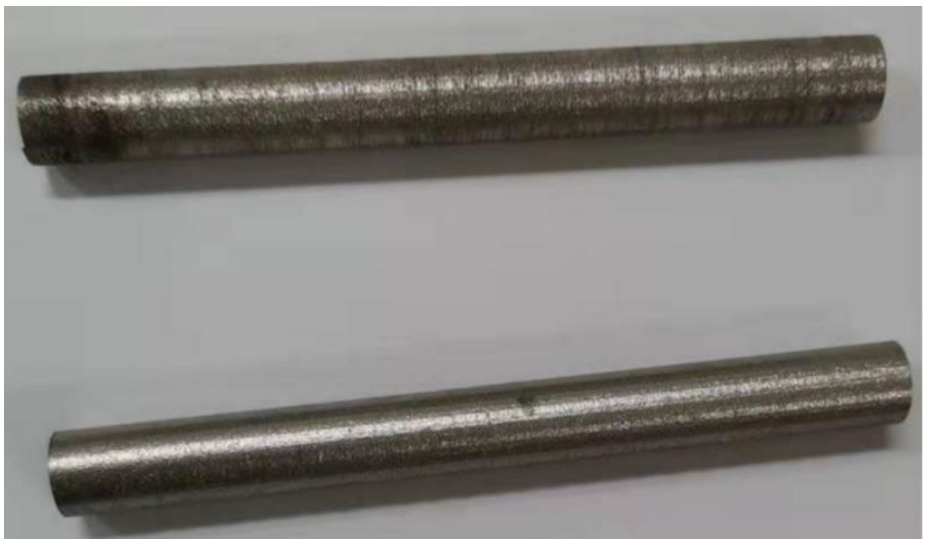

Figure 3. The printed sample

The HIP process is carried out on the sample after SLM forming. The equipment used is HIPEX80 produced by our company. The HIP parameters used are shown in Table 3 with a variety of different temperature and pressure combinations.

Materials Research Proceedings 38 (2023) 67-77 https://doi.org/10.21741/9781644902837-11

Table 3. HIP parameters

Number	Temp [℃]	Pressure/±5[MPa]	Soaking time[h]	Number	Temp [℃]	Pressure/±5[MPa]	Soaking time[h]
1	1100	135	4	7	1165	135	4
2	1100	155	4	8	1165	155	4
3	1100	175	4	9	1165	175	4
4	1135	135	4	10	1180	135	4
5	1135	155	4	11	1180	155	4
6	1135	175	4	12	1180	175	4

The surface morphology of polished specimens was observed by an optical microscope. The microstructures of the samples were observed by JSM-IT300LV scanning electron microscope. The microhardness of samples was measured by a microhardness tester, and 5 points were measured for each sample, and the average value was taken. The electronic universal testing machine was used to test the tensile properties at room temperature. Three samples were measured in each group and the average value was taken.

3. Results and discussion

3.1 Microstructure in GH4169 alloy

3.1.1 SLM structure and phase composition

The microstructure of GH4169 superalloy sample after SLM molding is shown in Fig. 4. Figure 4a shows the longitudinal section of the SLM sample. It can be seen from Figure 4 that the molten pool has a periodic fish scale structure. Because during the rapid scanning process, the temperature of the metal powder rises rapidly and cools rapidly, and the heat of the melt dissipates to the substrate and the surrounding powder, gradually solidifying and crystallizing to form pits. As shown in Fig. 4b, there are crisscross pool boundaries in the cross section, indicating discontinuous scanning channels.

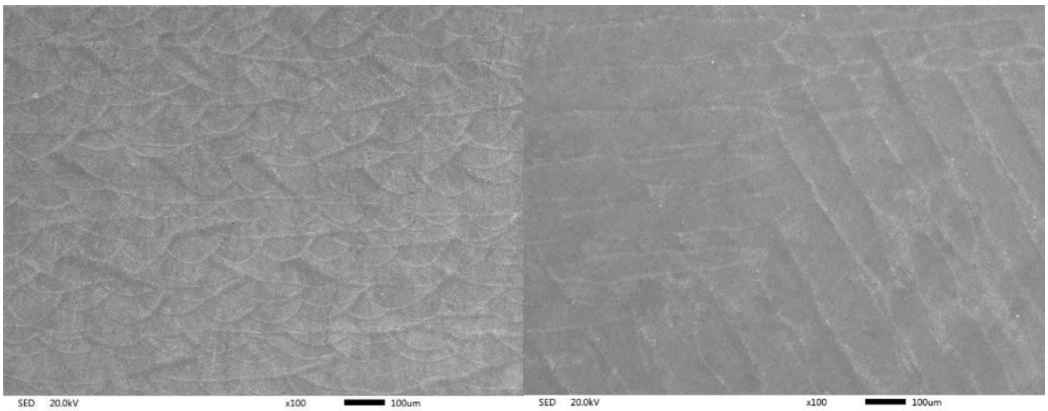

Figure 4. Structure of SLM sample a. longitudinal section(∥BD); b. cross section(⊥BD)

In the SLM structure, dendrites exhibit epitaxial growth (Fig. 5a), with small dendrite spacing of about 0.3-1.3μm. There are a large number of fine chain phases between the dendrites, as shown in Fig. 5a. The EDS spectrum shows that the fine interdendritic precipitates are Laves phase, as shown in Fig. 5b and Table 4. The dendrite spacing is inversely proportional to the product of molten pool temperature gradient and solidification rate. Eutectic products of γ+NbC and γ+Laves can form in the interdendritic region due to severe microscopic segregation, but the number of

Materials Research Proceedings 38 (2023) 67-77 https://doi.org/10.21741/9781644902837-11

γ+NbC eutectic is negligible compared to γ+Laves eutectic due to the very low carbon content in the material. Few other phases were observed except the Laves phase shown in Fig. 5a, presumably because rapid solidification inhibited their precipitation.

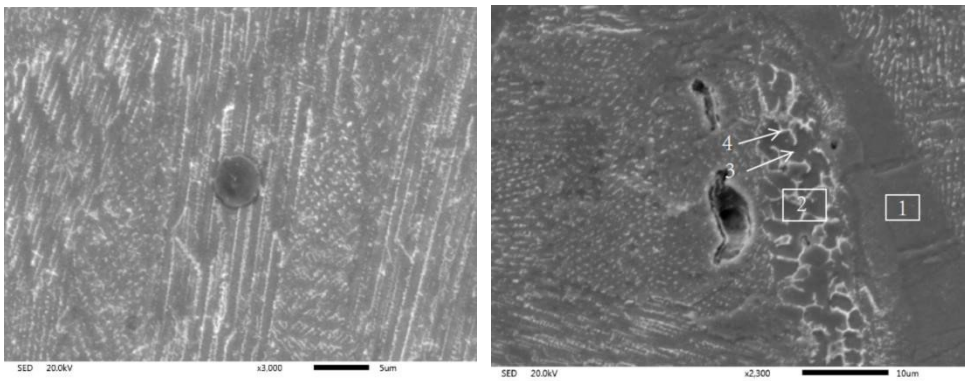

Figure 5. SLM dendrite structure

Table 4. The main chemical constituents of each phase in SLM state

Number	Phase	Ni	Cr	Fe	Nb	Mo	Ti	Al
1	γ	51.77	19.70	17.65	6.10	3.19	1.08	0.50
2	(γ+Laves) eutectic	50.51	19.45	17.61	7.25	3.69	1.08	0.41
3	γ in (γ +Laves) eutectic	52.08	20.36	19.20	3.56	3.33	0.92	0.55
4	Laves in (γ +Laves) eutectic	48.60	18.76	16.63	10.65	3.46	1.36	0.54

3.1.2 HIP structure and phase composition

Figure 6 and 7 show SEM images of cross section and longitudinal section of HIP samples respectively. At 1100℃, the microstructure of the sample still maintained columnar grain shape, and some recrystallization occurred, while some equiaxed crystals and a few twin crystals were observed. The chained Laves phase is dissolved, but the chained Laves phase and carbides are mainly distributed on grain boundaries. At 1135℃, the columnar grain morphology was almost invisible and twin crystals increased. The Laves phase is further dissolved, and most of them are granular. The Laves phase and carbides are distributed at grain boundary and in grain due to the transformation of microstructure. At 1165℃, recrystallization occurred in the sample, and a large number of twins were observed. The Laves phase is further dissolved and distributed evenly. At 1180℃, most grains of the samples grow together. The proportion of Laves phase continues to decrease, and Laves phase density areas exist locally due to grain consolidation and growth.

Materials Research Proceedings 38 (2023) 67-77 https://doi.org/10.21741/9781644902837-11

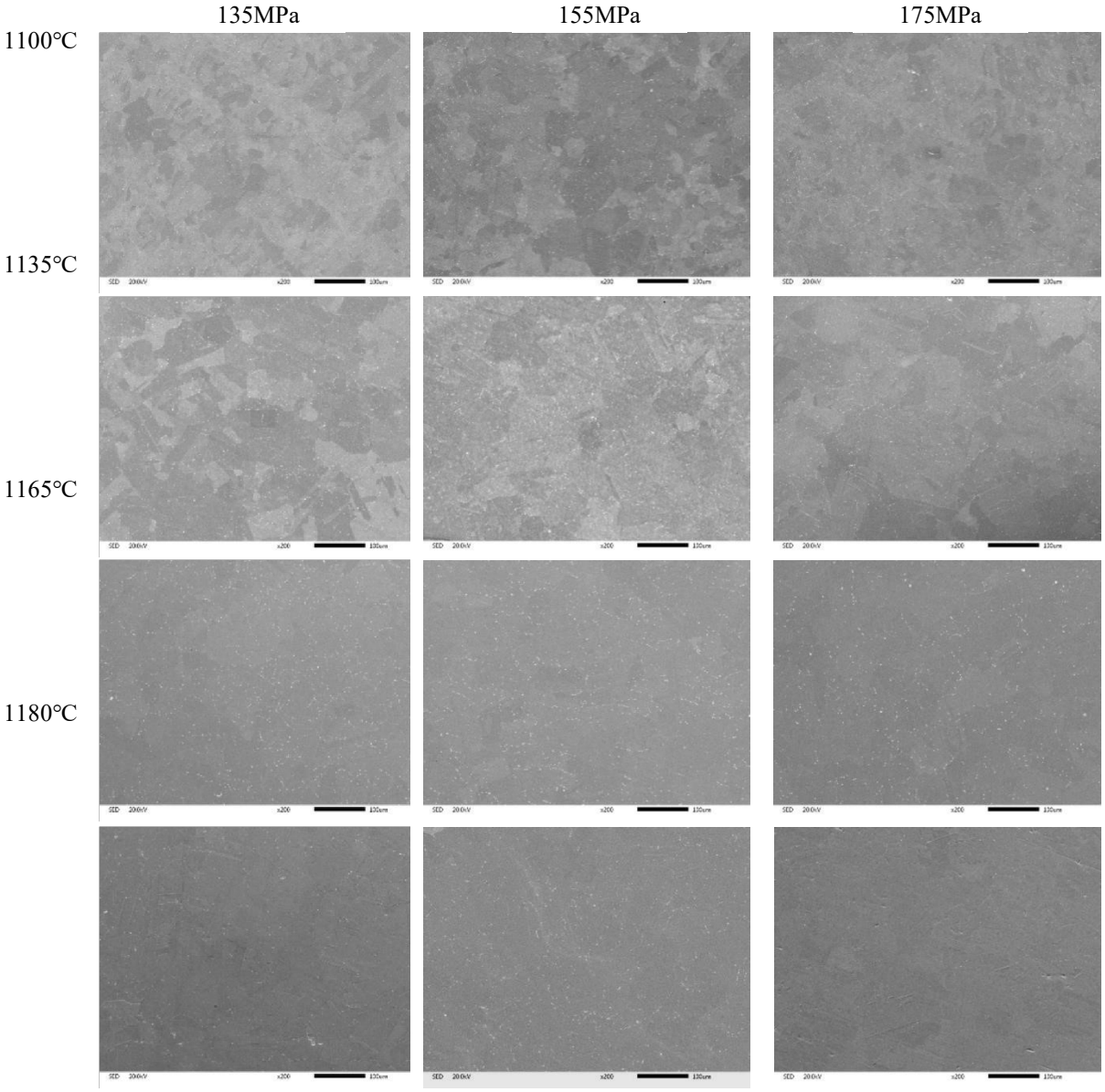

Figure 6. The microstructure of cross section (⊥ BD) of HIP specimen

Materials Research Proceedings 38 (2023) 67-77 https://doi.org/10.21741/9781644902837-11

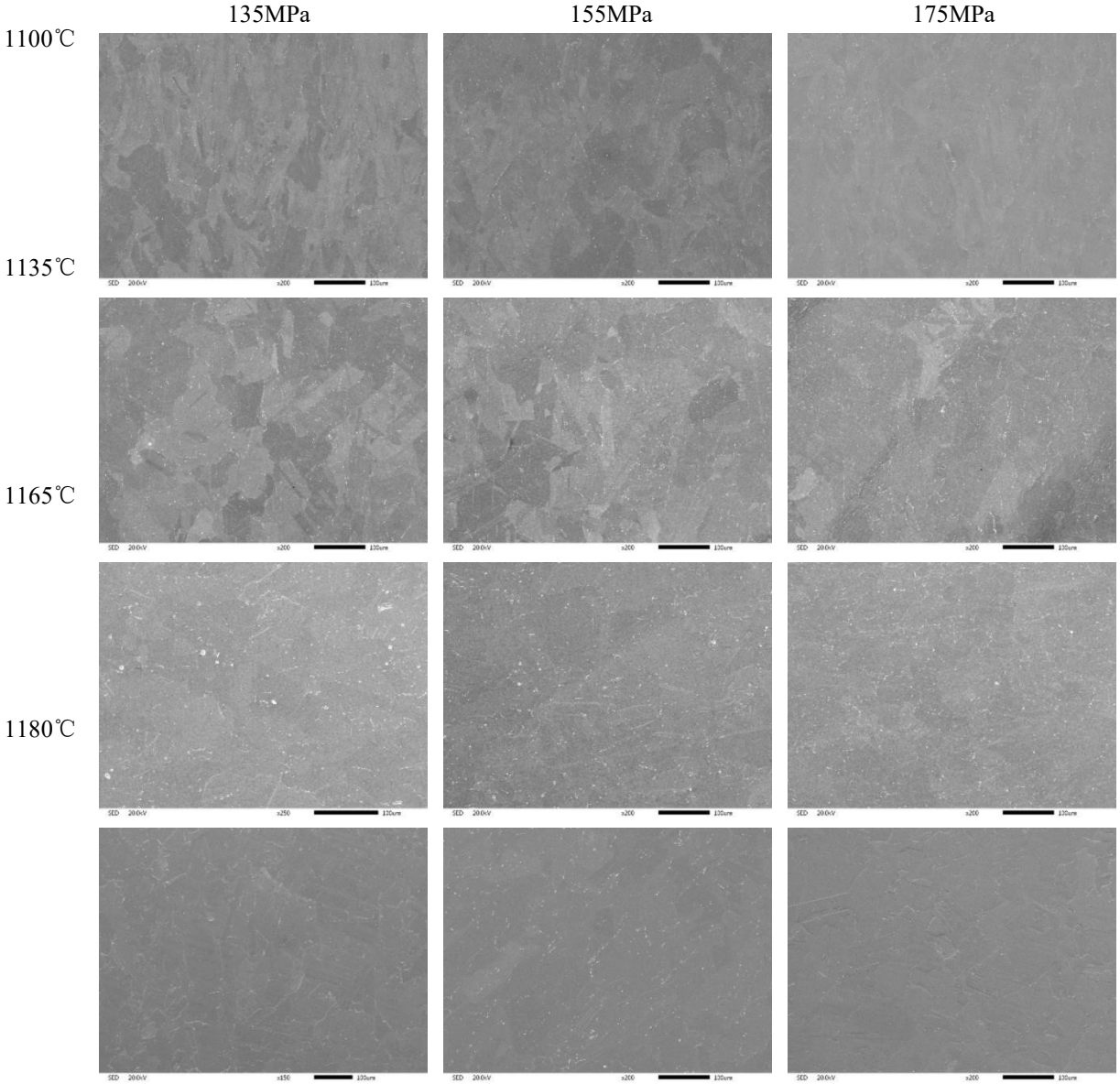

Figure 7. The microstructure of longitudinal section (∥BD) of HIP specimen

3.2 Microhardness and density

The microhardness of samples in different states was measured by EM500-2A semi-automatic micro Vickers hardness tester. The loading force was 1kg, the pressure holding time was 15s, and the spacing between two adjacent points was 1mm. Each piece was measured 5 times on the different positions, and the average value of each position was taken. The micro Vickers hardness of the cross section (⊥BD) of the sample after different HIP is shown in Fig. 8 After SLM molding, the microhardness of the sample is 315HV1. After HIP, the Vickers hardness of the sample decreases at other temperatures except 1100℃. The strengthening mechanism of SLM alloy is solid solution strengthening and carbide and Laves phase precipitation strengthening. Due to the rapid cooling rate of SLM process, the enhanced phase cannot be precipitated. After HIP, with the increase of HIP temperature, the Laves phase gradually dissolves and the strengthening ability decreases. Meanwhile, Nb, Mo and Ti elements are released from the Laves phase and diffused into the matrix, which improves the microstructure uniformity of the material and leads to the decrease of its microhardness.

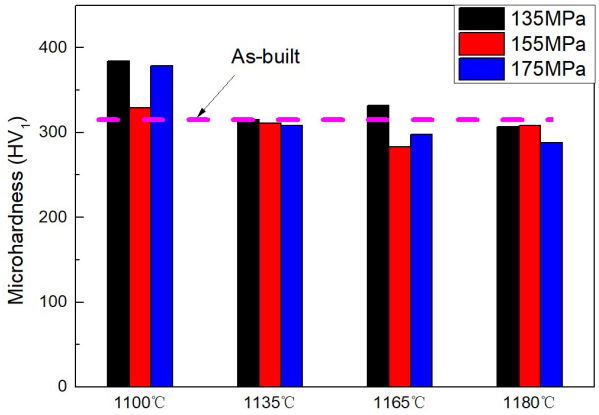

Figure 8. Microhardness of materials under different HIP treatments

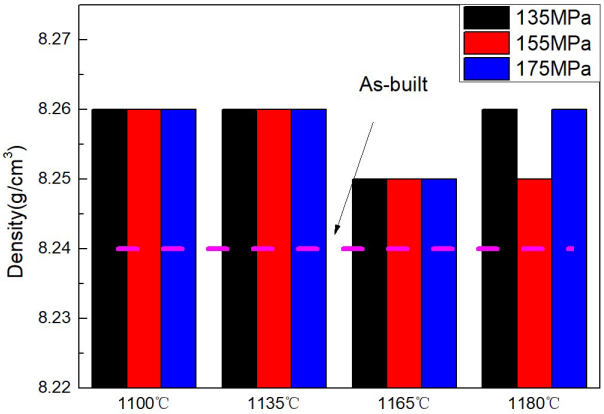

Figure 9. Material density under different HIP treatments

The density test results of the GH4169 alloy sample are shown in Fig. 9,SEM images show that the SLM sample has a small number of pores (as shown in Fig. 5), and no other defects are found. Its density is 8.24g/cm^3, and the density after HIP is 8.25-8.26g/cm^3, with no obvious change in density. The density of deformed parts of GH4169 given in *handbook of aeronautical materials of china* vol.2 is 8.24g/cm^3, indicating that the printed density is already very high, so the sample density does not increase significantly after HIP.

3.3 Tensile property

Figure 10 shows the tensile properties of SLM specimens treated by different HIP treatments. It can be seen from the figure that the tensile strength and yield strength of the specimens decrease gradually with the increase of HIP temperature, while the elongation presents an opposite trend. At 1100℃, the tensile strength and yield strength of the sample are significantly higher than those at the other three temperatures, while the elongation is significantly lower than those at the other three temperatures, which is related to the higher volume fraction of Laves phase and dislocation level of the sample at 1100℃. The strengthening mechanism of GH4169 material is solid solution strengthening and precipitation strengthening, so 1100℃ should be excluded. At HIP temperature of 1135℃, tensile strength and yield strength are relatively stable under various pressures, and the rate of strength change is the lowest at 135MPa, 155MPa and 175MPa, while elongation increases at 155MPa. At HIP temperature of 1165℃, the tensile strength and yield strength of the sample at 135MPa and 155MPa were higher than those at HIP temperature of 1135℃ and 1180℃. At HIP temperature of 1165C and 175MPa, the tensile strength and yield strength of the sample were

Materials Research Proceedings 38 (2023) 67-77 https://doi.org/10.21741/9781644902837-11

between 1135℃ and 1180℃, and the elongation showed a linear increase trend. At HIP temperature of 1180℃, the tensile strength and yield strength of the sample were lower than those of the other three temperatures. The tensile strength and yield strength showed a trend of rising first and then decreasing at the three pressures, while the elongation showed an opposite trend. As the cooling rate of HIP is faster than that of aging, there is almost no precipitation or strengthening phase, so the tensile strength and yield strength of the sample after HIP are lower than the forging level, but the elongation is much higher than the forging level.

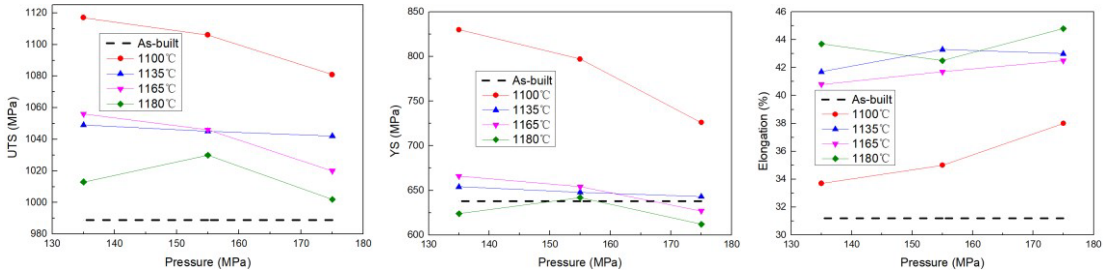

Figure 10. Tensile properties of SLM specimens treated by different HIP treatments

Figure 11 shows the tensile properties of SLM specimens treated by different HIP treatments. As shown in the figure, the tensile strength and yield strength of the specimens gradually decreased with the increase of HIP pressure, while the elongation showed an opposite trend. At HIP pressure of 175MPa, the tensile strength and yield strength of the sample continued to decrease, and were lower than those at 135MPa and 155MPa. The elongation of the sample at 1135℃ was slightly lower than that at 155MPa. When the HIP pressure is 135MPa and 155MPa, the tensile strength and yield strength of the sample show a decreasing trend with the increase of HIP temperature. At 1100℃, 1135℃ and 1165℃, the tensile strength and yield strength of the sample at 155MPa are lower than those at 135MPa. At 1180℃, the tensile strength of the sample at 155MPa is lower than that at 135MPa. The tensile strength and yield strength of the samples were higher than those at 135MPa. The values of tensile strength and yield strength of the samples reached the highest at 1165℃, excluding 1100℃. The elongation showed an opposite trend.

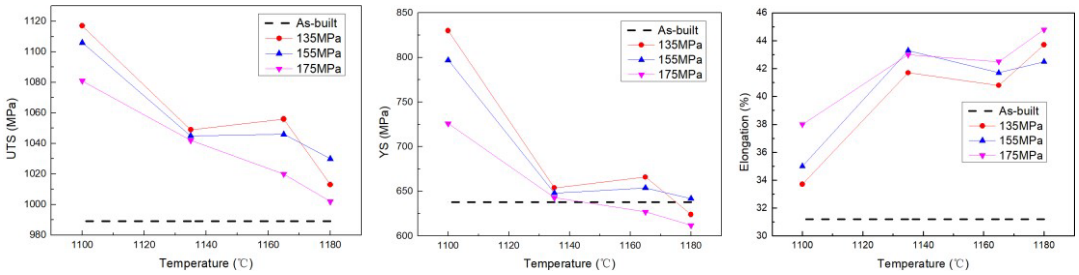

Figure 11. Tensile properties of SLM specimens treated by different HIP treatments

4. Conclusion and summary

The effects of different HIP treatments on the microstructure, SEM morphology, density, hardness and tensile properties of SLM GH4169 superalloy were investigated. The longitudinal section of SLM GH4169 superalloy is columnar grain with irregular shape, and the angle between grain and deposition direction is random. The average grain size is 10.5μm. The cross section grains are mainly equiaxed, with an average grain size of 5.93μm. In the SLM state, the dendrites are epitaxial growth with small dendrite spacing of 0.3~1.3μm. There are a lot of small chain Laves phases in the interdendrite. After HIP, the grain size of the sample increases and recrystallization occurs. Columnar grains transform into equiaxed grains on the longitudinal section. The Laves phase

gradually dissolves into granular form from the chain of SLM state. With the increase of recrystallization degree, the Laves phase is evenly distributed at the grain boundary and in the grain. There are a few pores in the SLM sample, and no other defects are found. The density of the sample is close to that of the deformed part, so the sample density does not increase significantly after HIP. With the increase of HIP temperature, the tensile strength and yield strength of the samples decreased gradually, while the elongation showed an opposite trend. With the increase of HIP pressure, the tensile strength and yield strength decrease gradually, while the elongation presents an opposite trend.

References

[1] K. Moussaoui, W. Rubio, M. Mousseigne, T. Sultan, F. Rezai.Effects of Selective Laser Melting additive manufacturing parameters of Inconel 718 on porosity, microstructure and mechanical properties, J. Materials Science and Engineering: A, 735 (2018) 182-190. https://doi.org/10.1016/j.msea.2018.08.037

[2] X. Li, J.J Shi, C.H Wang, G.H. Cao, A.M. Russell, Z.J. Zhou, C.P Li, G.F Chen. Effect of heat treatment on microstructure evolution of Inconel 718 alloy fabricated by selective laser melting, J. Journal of Alloys and Compounds, 764 (2018) 639-649. https://doi.org/10.1016/j.jallcom.2018.06.112

[3] D. Deng, R.L. Peng, H. Brodin, J. Moverare. Microstructure and mechanical properties of Inconel 718 produced by selective laser melting: Sample orientation dependence and effects of post heat treatments, J. Materials Science and Engineering: A, 713 (2018) 294-306. https://doi.org/10.1016/j.msea.2017.12.043

[4] M.T. Kim, S.Y. Chang, J.B. Won. Effect of HIP process on the micro-structural evolution of a nickel-based superalloy, J. Materials Science and Engineering: A, 441.1-2 (2016) 126-134. https://doi.org/10.1016/j.msea.2006.09.060

[5] S.H. Chang, S.C. Lee, T.P. Tang, H.H. Ho. Effects of temperature of HIP process on characteristics of Inconel 718 superalloy, J. International Journal of Cast Metals Research, 19.3 (2006) 175-180. https://doi.org/10.1179/136404606225023399

[6] K.N. Amato, S.M. Gaytan, L.E. Murr, E. Matinez, P.W Shindo, J. Hernandez, S. Collins, F. Medina. Microstructures and mechanical behavior of Inconel 718 fabricated by selective laser melting, J. Acta Materialia,60.5 (2012) 2229-2239. https://doi.org/10.1016/j.actamat.2011.12.032

[7] W. Tillmann, C. Schaak, J. Nellesen, M. Schaper, M.E. Aydinoez, K.P Hoyer. Hot Isostatic Pressing of IN718 Components Manufactured by Selective Laser Melting, J. Additive Manufacturing, 13 (2017) 93-102. https://doi.org/10.1016/j.addma.2016.11.006

[8] M. Muhammad, P. Frye, J. Simsiriwong, S. Shao, N. Shamsaei. An investigation into the effects of cyclic strain rate on the high cycle and very high cycle fatigue behaviors of wrought and additively manufactured Inconel 718, J. International Journal of Fatigue,144 (2021) 10638. https://doi.org/10.1016/j.ijfatigue.2020.106038

[9] J.N. DuPont, A.R. Marder, M.R. Notis, C.V. Robino. Solidification of Nb-bearing superalloys: Part II. Pseudoternary solidification surfaces, J. Metallurgical and Materials Transactions A, 29.11 (1998) 2797-2806. https://doi.org/10.1007/s11661-998-0320-x

[10] G.D. Janaki Ram, A. Venugopal Reddy, K. Prasad Rao, G. Madhusudhan Reddy. Control of Laves phase in Inconel 718 GTA welds with current pulsing, J. Science and technology of welding and joining, 9.5 (2004) 390-398. https://doi.org/10.1179/136217104225021788

[11] A.R. Balachandramurthi, N.R Jaladurgam, C. Kumara, T. Hansson, J.Moverare, J. Gardstam, R. pederson. On the Microstructure of Laser Beam Powder Bed Fusion Alloy 718 and Its Influence on the Low Cycle Fatigue Behaviour, J. Materials, 13.22 (2020) 5198. https://doi.org/10.3390/ma13225198

[12] Y. Kang, S. Yang, Y. Kim, B. AlMangour, K. Lee. Effect of post-treatment on the microstructure and high-temperature oxidation behaviour of additively manufactured inconel 718 alloy, J. Corrosion Science, 158 (2019) 108082. https://doi.org/10.1016/j.corsci.2019.06.030

[13] P.L. Blackwell. The mechanical and microstructural characteristics of laser-deposited IN718, J. Journal of Materials Processing Technology, 170.1-2 (2005) 240-246. https://doi.org/10.1016/j.jmatprotec.2005.05.005